

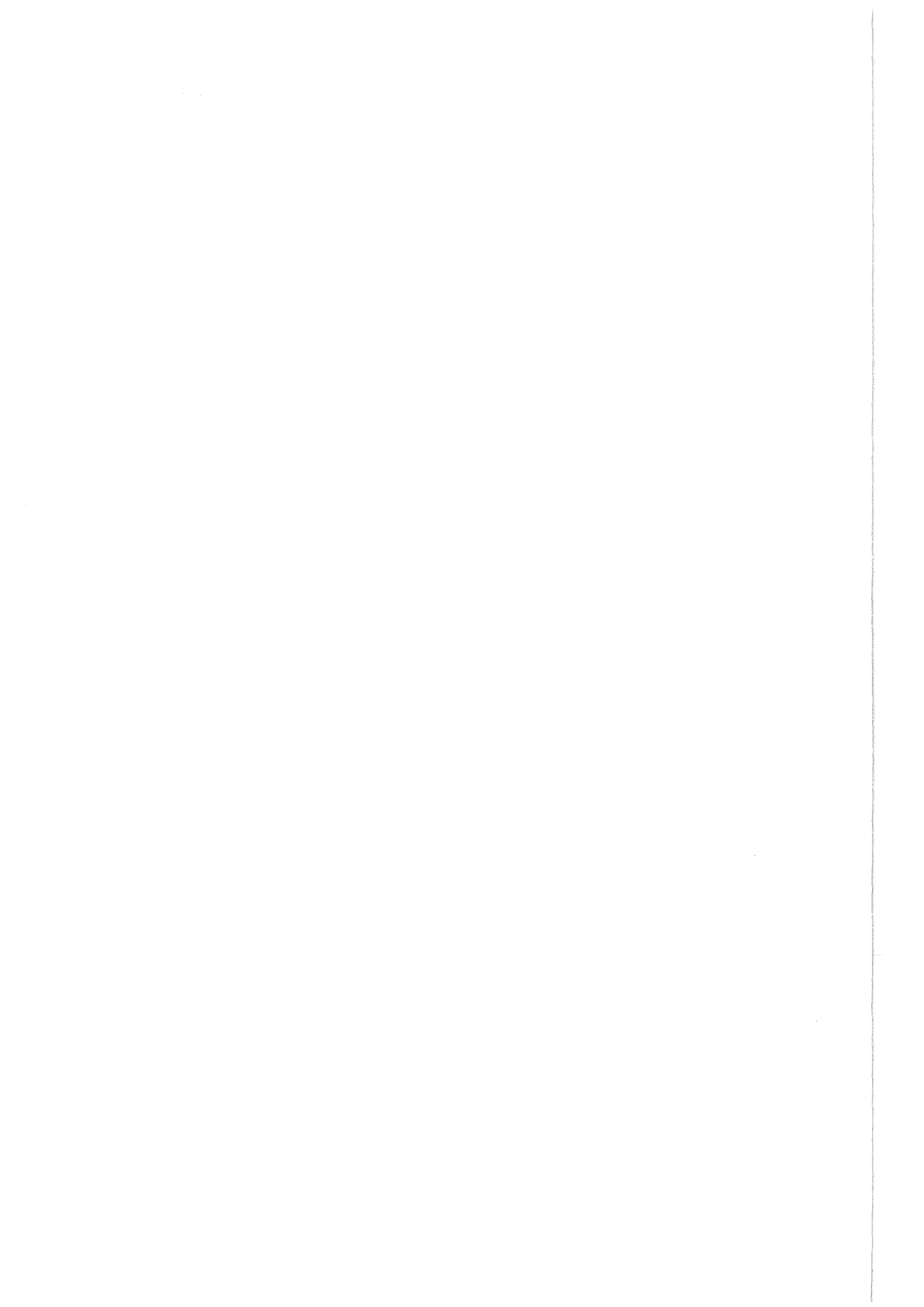
Forschungszentrum Karlsruhe
Technik und Umwelt

Wissenschaftliche Berichte
FZKA 5771

Coulomb Breakup of Nuclei-Applications to Astrophysics

G. Baur, H. Rebel
Institut für Kernphysik

April 1996



Forschungszentrum Karlsruhe

Technik und Umwelt

Wissenschaftliche Berichte

FZKA 5771

**Coulomb Breakup of Nuclei-Applications to
Astrophysics**

G. Baur* and H. Rebel

Institut für Kernphysik

*** Forschungszentrum Jülich, Institut für Kernphysik**

Forschungszentrum Karlsruhe GmbH, Karlsruhe

1996

Als Manuskript gedruckt
Für diesen Bericht behalten wir uns alle Rechte vor

Forschungszentrum Karlsruhe GmbH
Postfach 3640, 76021 Karlsruhe

ISSN 0947-8620

Abstract

The Coulomb dissociation process, induced by the intense source of quasi-real photons acting as nuclear particles passing the field of a heavy nucleus, has attracted a great deal of attention. As specific application and access to information to the "time-reversed" radiative capture reactions of astrophysical interest at stellar energies, it provides several advantages based on larger cross sections and on the flexibilities of the breakup kinematics. Difficulties in the analysis arise from possible interference of nuclear interactions and final state effects through multiphoton exchange ("post acceleration") which need careful consideration.

Since the introduction of this novel approach as tool of nuclear astrophysics, a number of theoretical and experimental investigations have been performed, with interesting new information and results which provide an improved and detailed understanding of the experimental conditions and of the theoretical basis of the method. The progress in experiment and theory is reviewed, and various cases of actual interest and current applications are discussed.

COULOMB-AUFBRUCH VON KERNEN - ANWENDUNGEN IN DER ASTROPHYSIK

Coulomb-Dissoziation, induziert von der intensiven Quelle quasi-reeller Photonen, die auf nukleare Teilchen einwirken, wenn sie das Feld eines schweren Kernes passieren, hat ein breites Anwendungsfeld gefunden. Als spezielle Anwendung in der nuklearen Astrophysik erlauben Coulomb-Dissoziations-Experimente den Zugang zu "zeitumgekehrten" Strahlungseinfangs-Reaktionen bei stellaren Energien. Dabei bieten sie verschiedene methodische Vorteile, dank großer Wirkungsquerschnitte und der Flexibilität der Dreiteilchen-Kinematik. Schwierigkeiten bei der Analyse ergeben sich aus der möglichen Interferenz mit der nuklearen Anregung des Kontinuums und der Endzustands-Wechselwirkung infolge des Vielphotonen-Austausches bei Prozessen höherer Ordnung. Seit der Einführung der neuen Methode in die experimentelle nukleare Astrophysik sind mehrere theoretische und experimentelle Studien durchgeführt worden, die ein verbessertes Verständnis der theoretischen Basis und der notwendigen experimentellen Bedingungen erlauben. Es wird ein Überblick über den Fortschritt in Experiment und Theorie gegeben. Verschiedene Fälle von aktuellem astrophysikalischen Interesse werden diskutiert.

CONTENTS

1. INTRODUCTION	1
2. THEORY OF ELECTROMAGNETIC EXCITATION AND DISSOCIATION	3
2.1 General	3
2.2 Inelastic scattering at high energies: one photon exchange and strong absorption, semiclassical approach and Glauber theory	5
2.3 Higher order electromagnetic effects: the ξ - χ plane, small ξ -approximation	9
3. EXPERIMENTAL SITES OF THE COULOMB DISSOCIATION APPROACH	13
4. SPECIFIC FEATURES OF ASTROPHYSICALLY RELEVANT CASES	19
4.1 Coulomb dissociation of ${}^6\text{Li}$ and ${}^7\text{Li}$	21
4.2 Dissociation of ${}^{11}\text{Li}$ and ${}^{11}\text{Be}$	22
4.3 The ${}^{14}\text{O} \rightarrow {}^{13}\text{N} + \text{p}$ Coulomb dissociation	23
4.4 The ${}^{12}\text{N} \rightarrow {}^{11}\text{C} + \text{p}$ Coulomb dissociation	23
4.5 Some cases which can be also useful as a test of the method: ${}^7\text{Be} \rightarrow \alpha + {}^3\text{He}$, ${}^{13}\text{N} \rightarrow {}^{12}\text{C} + \text{p}$, ${}^{17}\text{F} \rightarrow {}^{16}\text{O} + \text{p}$	23
4.6 Cases relevant for an inhomogeneous Big-Bang nucleosynthesis	25
4.7 Aspects and challenge of dissociation of ${}^{16}\text{O}$	26
4.8 ${}^8\text{B} \rightarrow {}^7\text{B} + \text{p}$ Coulomb dissociation and the Solar Neutrino Problem	27
5. CONCLUDING REMARKS	29
LITERATURE	31

1. INTRODUCTION

Nuclear astrophysics tries to understand how nuclear processes generate energy during the evolution of stars, and how, from primordial chemical abundancies, the rich distribution of nuclides as observed on the earth, in meteorites, in stars or in cosmic rays, is obtained.

The knowledge of certain nuclear reaction cross-sections is a key to explain cosmic processes, like the Big Bang, stellar evolution or supernova explosions (1, 2). Typically, one has to know cross-sections at very low collision energies corresponding to the relevant astrophysical temperatures. Their measurements in the laboratory, however, is often a rather difficult task since the required cross-sections are among the smallest. In most cases this is due to the Coulomb barrier between the charged nuclei, and reactions occur only after quantum mechanical tunneling. Such small cross-sections are experimentally accessible only with long data collection periods and painstaking attention to background and stability problems. A way out of the cosmic ray background problems is to go underground (3). The standard laboratory approach involves the bombardment of very thin targets with extremely low energy projectiles.

In addition, the electronic environment in astrophysical sites is usually different from that in the laboratory, and, in certain cases, it can be important to apply 'screening corrections'. In addition to the direct laboratory measurements, there are various indirect methods, which combine experimental results and theoretical analysis, with more or less theoretical bias. At the one extreme, there is the purely theoretical calculation of the weak interaction process $p + p \rightarrow d + e^+ + \nu_e$. Reactions, which proceed predominantly through a resonance, can often be studied completely satisfactorily in an indirect way, by e.g. producing the resonance in a suitable transfer reaction. In this way, e.g., the triple α -process, which proceeds by a resonance in the $\alpha + {}^8\text{Be}$ -system, is well known (4). Actually, such a resonance in the ${}^{12}\text{C}$ system was postulated before on purely theoretical arguments (5,6). On the other hand, the situation with the ${}^{12}\text{C}(\alpha, \gamma){}^{16}\text{O}$ reaction is still controversial. Another indirect method, the study of the α -decay following the β -decay of ${}^{16}\text{N}$ proved to be very useful (7, 8, 9).

In the present review, another indirect method, the Coulomb dissociation is discussed. The radiative capture reaction



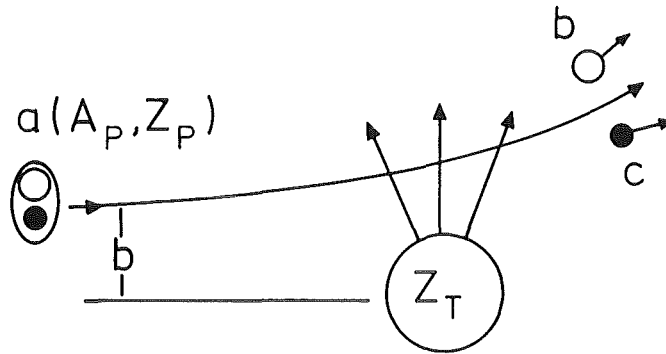


Fig. 1: Coulomb dissociation of a projectile $a \rightarrow b + c$ in the field of a target nucleus.

can also be studied as the time reversed reaction



at least in those cases, where the nucleus a is in the ground state. Now, the copious source of quasi-real photons provided by nuclei, especially heavy ones, has been useful in particle physics as well as nuclear physics: the so-called Primakoff effect (10), the electromagnetic excitation of relativistic projectiles in the field of (heavy) nuclei, has been a very useful source of information. A projectile passes through the Coulomb field of a nucleus, as shown schematically in Figure 1. It experiences a time-dependent electromagnetic field. This field is equivalent to a spectrum of quasi-real photons. In order to ensure that there is no strong interaction between the projectile and the target, one has two possibilities: one can choose a bombarding energy well below the Coulomb barrier. This is the very well known field of Coulomb excitation (see e.g. (11)). On the other hand, for higher energies, above or well above the Coulomb barrier, one can restrict oneself to small angles, which correspond, semiclassically, to trajectories where the nuclei do not touch each other. The study of low- as well as high lying nuclear states by means of electromagnetic excitation in the nuclear Coulomb field has been an extremely fruitful source of unambiguous information. The “double Primakoff-effect“ has been studied extensively at e^+e^- -colliders to obtain information on two photon physics. It is the purpose of this review to examine the applications of this method to astrophysical reactions. About a decade has passed since its proposal (12 - 14). In the Coulomb dissociation process



the cross-section for the reactions eq. (2) or, equivalently eq. (1), can be extracted by means of the equivalent photon method. The theoretical analysis, along with a discussion of disturbing effects, is discussed in Ch. 2. The experimental realization is studied in Ch. 3. Application to individual cases is given in Ch. 4, a conclusion and an outlook is given in Ch. 5. A ‘topical review’ was given by the present authors (15) about 3 years ago. By comparing the two papers, the progress in the field can be assessed.

2. THEORY OF ELECTROMAGNETIC EXCITATION AND DISSOCIATION

2.1 General

Electromagnetic excitation of nuclei has been studied experimentally and theoretically during the last decades. The theory is well understood, see e.g. (11). Due to the condition that projectile and target do not interpenetrate, the electromagnetic interaction can be parametrized in terms of electromagnetic matrix-elements at the photon point i.e. $|\vec{k}| \equiv k = \omega$. In contrast to this, the interaction of electrons and hadrons is determined by the exchange of a (spacelike) virtual photon, i.e. $k > \omega$.

In order to ensure the dominance of the long-range electromagnetic interaction over the short-range strong interactions, bombarding energies were usually chosen to be below the Coulomb barrier. The strength of the Coulomb interaction is measured by the Coulomb (Sommerfeld) parameter

$$\eta = \frac{Z_1 Z_2 e^2}{\hbar v} = \frac{a}{\lambda} \quad (2.1)$$

where a is half the distance of closest approach in a head-on collision and λ is the de Broglie wave-length. For $\eta \gg 1$ the projectile motion is well described classically by the Rutherford hyperbola. The condition of no penetration is then well fulfilled, provided that $2a > R_1 + R_2$, the sum of the nuclear radii. Since only low energy states can be appreciably excited, the condition that $\Delta E / E \ll 1$ for the semiclassical approximation to be valid, is also well fulfilled. E denote the beam energy and ΔE is the energy loss due to the excitation. If necessary, the virtual excitation of high lying states can be included by a polarization potential. Nuclear interactions between the projectile and target are always

present at a certain level, e.g. in the Sub-barrier fusion process. They can usually be neglected in the study of the electromagnetic excitation process.

In hadron-hadron scattering at high energies, well above the Coulomb barrier, there are always strong interactions between the projectile and the target. However, even in such a situation, one can have dominance of the electromagnetic interaction by going to very forward angles. The propagator for a zero mass particle (photon) contains the term $\frac{1}{q^2}$,

instead of $\frac{1}{q^2 + m^2}$, for a particle with mass m . In the limit of $q^2 \rightarrow 0$ the photon exchange

gives therefore the dominant contribution. In a Born approximation approach, the 4-momentum of the exchanged photon is given by the difference between the 4-momenta of the ingoing and outgoing particle. The limit $q^2 \rightarrow 0$ can be accompanied by a finite energy transfer ω . In the target rest frame, e.g., we have the photon 4-momentum $q = (\omega, \vec{q}_\perp, q_{\min})$

where $q_{\min} = \frac{\omega}{\gamma v}$. This leads to $q^2 = \left(\frac{\omega}{\gamma v}\right)^2 + \vec{q}_\perp^2$, the invariant mass of the exchanged

photon. It goes to zero for $\gamma \rightarrow \infty$ and $\vec{q}_\perp \rightarrow 0$ (i.e. for forward angles). Semiclassically, the limit $\vec{q}_\perp \rightarrow 0$ corresponds to large impact parameters b .

The angular distribution will be given by an interplay between Coulomb deflection and diffraction effects. The basic parameters are the Coulomb deflection angle θ_c and the diffraction angle θ_d .

It is the purpose of the next section to give an overview over the basic effects, in a qualitative as well as quantitative way. Since the details are well described and documented in the literature, we think that it is best to give here the main ideas and the key formulae. Also, computer codes exist which deal more specifically with electromagnetic excitation. Of course, there are also very elaborate computer codes, which deal with nuclear inelastic scattering in a general way. They are essentially based on fully quantal DWBA or coupled channels approaches. Yet, it is indispensable and very helpful to use other appropriate approximation methods to obtain a basic understanding of the physics.

2.2 Inelastic scattering at high energies: one photon exchange and strong absorption, semiclassical approach and Glauber theory

In contrast to lepton-nucleus scattering, there are also strong interactions between the colliding nuclei, in addition to the electromagnetic interaction. In the short wave-length limit, the c.m. motion of the nuclei can be treated classically. At high enough energies, it is sometimes a good enough approximation to take a straight-line trajectory, possibly with a suitable modification for the Coulomb repulsion between the nuclei. At a certain minimum impact parameter, strong absorption sets in more or less rapidly. This leads to a cut-off of the small impact parameters.

It is very instructive to study the non-relativistic straight-line limit in the electric dipole approximation. It is given explicitly in Ch. 19 of (16). The excitation amplitude is given by

$$a_{fi} = \frac{2Ze^2}{\hbar b v} \left(x K_1(x) D_{fi}^x + ix K_0(x) D_{fi}^z \right) \quad (2.2)$$

where $x = \frac{\omega b}{v}$ and K_n is the Bessel function of imaginary argument. The impact parameter b is chosen to be in the x -direction, and the velocity \vec{v} of the exciting nucleus (with charge number Z) in the z -direction. The corresponding components of the electric dipole matrix-element between the initial state i and final state f are denoted by D_{fi}^x and D_{fi}^z , respectively. Using the behavior of K_n for small and large argument we can write eq (2.2) approximately as

$$a_{fi} = \frac{2Ze^2}{\hbar b v} D_{fi}^x \quad \text{for } b < \frac{v}{\omega}$$

and

$$a_{fi} = 0 \quad \text{for } b > \frac{v}{\omega} \quad (2.3)$$

Eq (2.3) is a very useful guide in many practical cases. This semiclassical approach has been generalized in different ways:

- (i) Especially for low relative velocities, it is important to take Coulomb repulsion into account and replace the straight lines by Rutherford trajectories. The electric dipole case is also generalized to arbitrary electromagnetic multipoles $\pi\gamma$ ($\pi = E, M$; $\lambda = 1, 2, 3, \dots$). The electric dipole strength in nuclei is located so high in general, that

$a_{fi} \cong 0$ for such excitations. Thus the interest is focussed on low lying rotational and vibrational states. For a review, see (11).

- (ii) The straight-line motion of the nuclei is treated relativistically, and all electromagnetic multiplicities are considered. A beautiful analytical result was found in (17). The excitation amplitude is given by

$$a_{fi} = -i \frac{Ze}{\gamma \hbar v} \sum_{\pi\lambda\mu} (-1)^\mu \sqrt{2\lambda+1} \left(\frac{\omega}{c}\right)^\lambda G_{\pi\lambda\mu} \left(\frac{c}{v}\right) K_\mu \left(\frac{\omega b}{\gamma v}\right) \langle I_f M_f | M(\pi\lambda, -\mu) | I_i M_i \rangle \quad (2.4)$$

The functions $G_{\pi\lambda\mu}$ can be expressed in terms of the associated Legendre polynomials. The dependence on the kinematics of the process and on the nuclear properties are clearly separated. A correction for the Coulomb repulsion is also given in (17). In this case, the integration over impact parameters has to be done with care (18).

- (iii) Generally one has to cope with the Coulomb repulsion and the relativistic effects simultaneously. For the electric dipole case, a convenient interpolation procedure is suggested in (13,19). The general case is treated in (20). The formulae given there can be readily used in computer codes.

The finite wave-length of the projectile gives rise to diffraction effects. This leads to deviations from the semiclassical approximation. For the high energy collisions they are most conveniently studied in the Glauber approach. We follow the formulation given in (21). It reveals qualitatively the dependence of the effects on the basic parameters. The incident projectile, nucleus 1, excites the target nucleus 2, while the projectile remains in the ground state. The strong interaction between the nuclei enters via the eikonal wave functions for the distorted waves, i.e.

$$\phi_{\vec{k}'}^{(-)}(\vec{r}) \phi_{\vec{k}}^{(+)}(\vec{r}) = e^{-i\vec{q}\cdot\vec{r} + i\chi(b)} \quad (2.5)$$

where $\vec{q} = \vec{k}' - \vec{k}$ and

$$\chi(b) = \frac{-1}{\hbar v} \int_{-\infty}^{\infty} dz' U_N(z', b) + \Psi_c(b) \quad (2.6)$$

The nuclear optical potential is given by U_N and the Coulomb phase is denoted by $\Psi_c(b)$.

The main features can be seen in a black disk model, i.e. we put

$$\begin{aligned}
e^{i\chi(b)} &= 0 & b < R \\
e^{i\eta \log(kb)} & & b > R
\end{aligned} \tag{2.7}$$

In this sharp cut-off model the divergence of the pure Coulomb phase for $b \rightarrow 0$ does not matter.

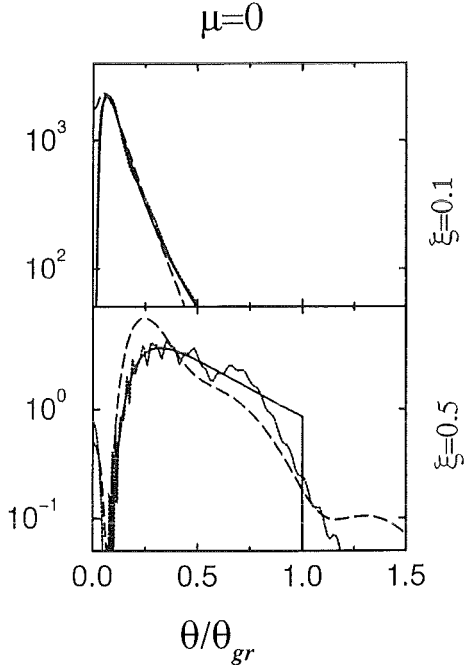


Fig. 2: The quantity $\left| \Omega_\mu \frac{2\eta}{R^2} \right|^2$ (see eq. 2.9) is plotted as a function of the reduced angle variable $\theta_{red} = \theta / \theta_{out}$ for $\mu = 0$. In the top part, the adiabaticity parameter is given by $\xi = 0.1$, the dashed line corresponds to $\eta = 1.2$, the dotted line to $\eta = 3$ and the continuous line denotes the semiclassical limit $\eta \rightarrow \infty$ (see eq. 2.10). In the bottom part, the adiabaticity parameter is given by $\xi = 0.5$, the dashed line corresponds to $\eta = 2$, the dotted line to $\eta = 20$ and the continuous line denotes the semiclassical limit.

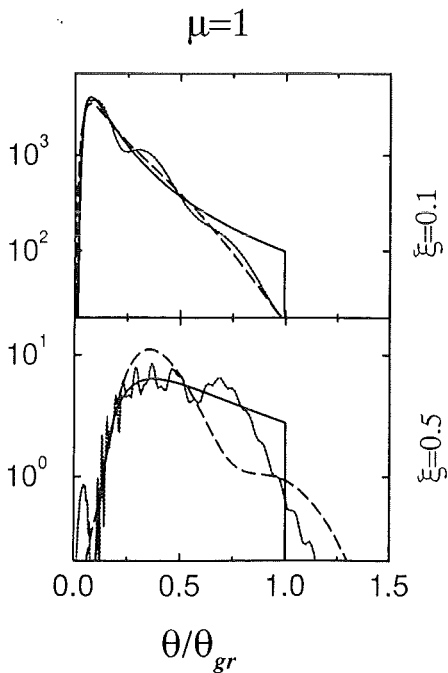


Fig. 3: The same as in Figure 2 for $\mu = 1$.

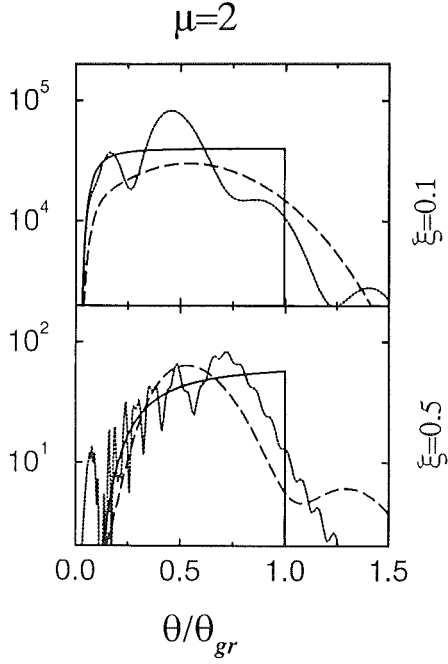


Fig. 4: The same as in Figure 2 for $\mu = 2$.

The interaction which leads to the target excitation is assumed now to be pure electromagnetic. The scattering amplitude can now be written as (see eq. 7 of (21)).

$$f(\theta) = i \frac{Z_1 e k}{\gamma \hbar v} \sum_{\pi \lambda \mu} i^\mu \left(\frac{\omega}{c} \right)^\lambda \sqrt{2\lambda + 1} e^{i\mu\phi} \Omega_\mu(\mathbf{q}) G_{\pi \lambda \mu} \left(\frac{c}{v} \right) \langle I_f M_f | M(\pi \lambda, -\mu) | I_i M_i \rangle \quad (2.8)$$

The factor $\Omega_\mu(\mathbf{q})$ determines the angular distribution. It is given by

$$\Omega_\mu(\mathbf{q}) = \int_R^\infty db b J_\mu(qb) K_\mu \left(\frac{\omega b}{\gamma v} \right) e^{2i\eta \log(kb)} \quad (2.9)$$

In the small-angle approximation, which we can safely use for the present discussion, the perpendicular momentum transfer is given by $q = k\theta$. We introduce the Coulomb grazing angle $\theta_{\text{Coul}} = 2\eta\theta_{\text{diff}}$, the diffraction angle $\theta_{\text{diff}} = \frac{1}{kR}$. Apart from an unimportant constant phase factor, eq (2.9) can be written as

$$\Omega_\mu(\mathbf{q}) = R^2 \int_1^\infty du u J_\mu \left(\frac{\theta}{\theta_{\text{diff}}} u \right) K_\mu(\xi u) e^{2i\eta \log u} \quad (2.9')$$

The total cross-section can be obtained by using the small angle approximation $d\Omega \cong 2\pi \frac{dq}{k^2}$ and the closure relation for the Bessel function (see e.g.(21)). It seems interesting to note that this quantity is independent of the Coulomb parameter η . On the other hand, the

angular distribution depends very sensitively on it. In Figures 2-4 the quantity $\left| \Omega_{\mu} \frac{2\eta}{R^2} \right|^2$ is shown, for various values of ξ and η as a function of the „reduced“ angle variable $\theta_{\text{red}} = \theta / \theta_{\text{Coul}}$. The case $\eta = 0$, which corresponds to a neutral particle (e.g. Λ°) has been given analytically in (19). The limit $\eta \rightarrow \infty$ corresponds to the semiclassical case it is given by

$$\left| \Omega_{\mu}^{\text{s.cl.}} \frac{2\eta}{R^2} \right|^2 = \theta_{\text{red}}^{-4} \left| K_{\mu} \left(\frac{\xi}{\theta_{\text{red}}} \right) \right|^2. \quad (2.10)$$

For finite values of η , one can observe the influence of the wave character of the projectile in Figures 2-4. For further discussion see (22).

2.3 Higher order electromagnetic effects: the ξ - χ -plane, small ξ -approximation

For slow collisions below or around the Coulomb barrier, higher order electromagnetic effects are a common and useful feature, especially with heavy ion projectiles. With increasing relative velocity, the importance of these higher order effects diminishes, but they do not vanish altogether. It is the purpose of this section to show how one can take higher order effects into account for the fast transitions in an appropriate way.

The strength parameter $\chi^{(\lambda)}$ measures the number of photons exchanged in a transition with multipolarity $E\lambda$. It is given by (see (11))

$$c^{(l)} = \frac{1}{\hbar} \int dt \langle f | V_{\text{int}} | i \rangle \cong \frac{e \langle f | M(E1) | i \rangle}{\hbar c b^l} \left(\frac{c}{v} \right) \quad (2.11a)$$

The strength parameter is inversely proportional to velocity. In slow collisions, there is just more time to exchange photons. Another important parameter is the adiabaticity parameter ξ , the ratio between collision time and nuclear excitation time. It is given by (see (11))

$$\xi = \frac{\omega b}{v} \quad (2.11b)$$

If $\chi^{(\lambda)}$ is much less than one, it is often sufficient to use the 1st order amplitude

$$a_{fi}^{(1)} = \frac{1}{i\hbar} \langle f | \int_{-\infty}^{\infty} dt e^{i\omega t} V(t) | i \rangle \quad (2.12)$$

On the other hand, if we have $\xi \ll 1$, one can use the sudden approximation for all values of the strength parameter $\chi^{(\lambda)}$. One can then neglect the time-ordering in the perturbation expansion and sum up the interactions to infinite order. One obtains (see e.g. (11))

$$a_{fi}^{sa} = \langle f | \exp\left(\frac{1}{i\hbar} \int_{-\infty}^{\infty} dt V(t) \right) | i \rangle \quad (2.13)$$

Thus a new operator, different from the electromagnetic operators, appears between the states $|i\rangle$ and $|f\rangle$. Depending on the given situation, one can try to evaluate this matrix-element directly, or one can expand the exponential in a power series of $V(t)$. In this case, the usual electromagnetic matrix-elements appear, but now (at least principle) between all intermediate states.

When v gets smaller, $\chi^{(\lambda)}$ as well as ξ will increase and the sudden approximation will become poor. In a ξ - χ - plane the „tractable“ regions are $\xi \ll 1$ (sudden) and $\chi^{(\lambda)} \ll 1$ (1st order). From eqs. (2.10) and (2.11) we have

$$\chi^{(\lambda)} = C_{\lambda} \xi^{-\lambda} \quad (2.14)$$

with the dimensionless parameter

$$C_{\lambda} = \frac{e \langle f | M(E\lambda\mu) | i \rangle}{\gamma^{\lambda} \hbar c} \left(\frac{\omega}{c}\right)^{\lambda} \left(\frac{c}{v}\right)^{\lambda+1} \quad (2.14')$$

If C_{λ} is small enough, the 1st order region, with $\chi^{(\lambda)} < 1$ and the sudden region, with $\xi < 1$ are joined together when b varies from its minimum value b_{\min} (with a corresponding $\chi_{\max}^{(\lambda)}$ and ξ_{\min}) to infinity. If C_{λ} is large, $C_{\lambda} > 1$, then one will have to use more elaborate methods. In such a case, it seems not so clear how one can extract certain electromagnetic matrix-elements in a model-independent way. An application of these consideration to the excitation of the 1st excited state in ^{11}Be is given in (23). For the beam energy of 45 MeV/A, corresponding to a recent experiment at GANIL (24), the parameter C_{λ} is much less than one. With a minimum of nuclear model assumption, a good theoretical understanding of the importance of higher order effects is obtained in this case (23). Notably, there is a

discrepancy between the theoretical predictions (23) and the experimental results (24). The future will tell us more about the reliability of both results.

There are various ways to deal with the more general situation, where C_λ is not very much smaller than one. Which of the methods is most suitable will depend to some extent on the given special case.

One well known and well developed approach is the coupled channels method. One picks out a certain number of nuclear states considered to be relevant. The corresponding electromagnetic matrix-elements between those states enter as parameters in such a calculation. A recent example is given in (25), where the conclusion about the electromagnetic excitation of the 1st excited state in ^{11}Be are similar to those in (23). However, stronger assumptions about nuclear structure have to be made in the coupled channels approach.

Another method is the direct numerical solution of the time-dependent Schrödinger equation. Up to now, only rather simple model Hamiltonians have been used (26 - 28). The extension of this method to realistic nuclear Hamiltonians remains to be seen.

The method of the small ξ -approximation was developed recently (29, 30). It leads to an expression which is of 2nd order in the electromagnetic interaction and is valid for small values of ξ . It extends the region of the validity of the sudden approximation. Due to the long range of the Coulomb potential higher order terms can diverge. This is not so serious since, usually, we can stop at the 2nd order (see also a similar approach in (11) p. 184). In contrast to the usual 2nd order calculation, intermediate states do not appear explicitly. Instead, one has a matrix-element of an effective operator between the initial and final states in question.

This can be an enormous simplification, since the wave functions of the intermediate states and the corresponding electromagnetic matrix-elements may not be well known. So the small ξ -approximation can be a step towards a model-independent analysis of experimental data.

Suppose e.g. that a set of data is available at different beam energies. Assuming that the small ξ -approximation is valid, the excitation amplitude for a given transition from i to f can be expressed in terms of a few parameters, the matrix-elements of certain operators between the states i and f . We can write the amplitude as a sum of a 1st and 2nd order term,

$$\mathbf{a}_{fi} \cong \mathbf{a}_{fi}^{(1)} + \mathbf{a}_{fi}^{(2)} \quad (2.15)$$

where $\mathbf{a}_{fi}^{(1)}$ is given by (2.12). Expanding the perturbation $V(t)$ into multipoles, one obtains in the standard way

$$\mathbf{a}_{fi}^{(1)} = 4\pi \frac{Ze}{i\hbar} \sum_{\pi\lambda\mu} \frac{(-1)^\mu}{2\lambda+1} \langle f | \mathbf{M}(\pi\lambda - \mu) | i \rangle S_{\pi\lambda\mu}(\omega) \quad (2.16)$$

The orbital integrals $S_{\pi\lambda\mu}(\omega)$ are well known, see e.g. (1). The electromagnetic multipole matrix-element is the quantity of interest. The 2nd order amplitude is given by eq. 24 of (30):

$$\mathbf{a}_{fi}^{(2)} = \left(4\pi \frac{Ze}{i\hbar}\right)^2 \sum_{\mu} \frac{(-1)^\mu}{(2\lambda'+1)^2} * \left\{ \frac{1}{2} \langle f | \mathbf{N}_{EE}^{\lambda'\lambda'}(\lambda - \mu) | i \rangle \left(\mathbf{T}_{\lambda\mu}^{E\lambda'E\lambda'}(\omega, \omega) + \xi \mathbf{U}_{\lambda\mu}^{E\lambda'E\lambda'}(\omega, \omega) \right) - \frac{\mathbf{a}}{v\hbar} \right.$$

$$\left. \langle f | \mathbf{K}_{EE}^{\lambda'\lambda'}(\lambda - \mu) | i \rangle * \frac{i}{\pi} \mathbf{P} \int_{-\infty}^{\infty} \frac{d\mathbf{q}}{q} \mathbf{U}_{\lambda\mu}^{E\lambda'E\lambda'}(\omega - \mathbf{q}, \omega + \mathbf{q}) \right. \quad (2.17)$$

Here we restricted ourselves to the case of one electric multipolarity $\lambda' = \lambda_1 = \lambda_2$. The slightly more general case with different multiplicities λ_1 and λ_2 is given by eq. 23 of (30). The new multipole operators $\mathbf{N}_{\pi_1\pi_2}^{\lambda_1\lambda_2}$ and $\mathbf{K}_{\pi_1\pi_2}^{\lambda_1\lambda_2}$ as well as the orbital integrals $\mathbf{T}_{\lambda\mu}^{\pi_1\lambda_1\pi_2\lambda_2}$ and $\mathbf{U}_{\lambda\mu}^{\pi_1\lambda_1\pi_2\lambda_2}$ are also given there. The orbital integrals are well known from the kinematics of the process. This will help to disentangle the electromagnetic matrix-elements and the matrix-elements of the new operators \mathbf{N} and \mathbf{K} (again only between the states i and f) from each other in a model-independent way.

The small ξ -method was applied to the case of ^8B Coulomb dissociation (30). Assuming a more or less reasonable model for the wave functions of ^8B , the matrix-elements of the effective operators were evaluated. It was concluded that the effects of the 2nd order electromagnetic interaction („post-acceleration“) are rather small at the RIKEN beam energies ($\approx 50 \text{ MeV} / \text{A}$). When more experimental data for different beam energies become available, such a model-independent approach can become very useful, and consistency checks are possible. Such relatively simple procedures would be obscured by more complicated types of analysis, e.g. a coupled channels approach, with the many necessary free input parameters.

Finally, at low energies, one tends to have $\xi \gg 1$ and $\chi \gg 1$. This case will not be very useful from the present point of view, where one wants to extract the electromagnetic matrix-

element for the transition from i to f . In this case, the excitation probability is small. Transitions can occur at the near crossing of adiabatic energy levels. While very important in atomic physics for example, it seems difficult to realize this limiting case in nuclear physics and, in addition, it seems quite impossible to extract information on the wanted electromagnetic matrix-elements.

3. EXPERIMENTAL SITES OF THE COULOMB DISSOCIATION APPROACH

The Coulomb dissociation approach is preferably applicable to projectiles with low particle decay thresholds and with a relatively simple level structure. Such conditions are met for example with exotic nuclei far off stability and they favour the use of radioactive particle beams. Experimentally it requires the observation of near-parallel emission of the ejectiles of binary breakup of the fast projectiles in very forward angles, determining the triple differential cross sections $d^3\sigma / dE_c d\Omega_{b(c)}$ in a kinematically complete experiment.

Table 1: Aspects of high projectile energies

Advantages:

Small ξ values - higher dissociation threshold accessible

Generally increased dissociation probabilities

Improved energy resolution on the relative-energy scale: ‘Magnifying glass effect’

Reduced dispersion (‘post-acceleration’) in the Coulomb field

Semi-classical description valid

Thicker targets admissible

Disadvantages:

Shrinking the forward angular range for Coulomb scattering

Narrow detector geometry and necessity of increased angular accuracy and resolution

Larger background from competing processes in forward direction

The choice of the most suitable conditions in projectile energy and of angular region for observation needs a careful consideration of the specific features of each particular case, along the arguments of minimising disturbances from the interference of nuclear interactions and higher-order processes. In general, large projectile energies are to be preferred (Table 1). They assure the non-adiabacity condition

$$\xi(b) = \frac{\omega \cdot b}{\gamma \cdot v} \ll 1 \quad (3.1)$$

which guarantees the dominance of Coulomb excitation at $E_x = \hbar \cdot \omega$, and they relieve the problems arising from post-acceleration effects since the strength parameter ξ decreases. High projectile energies, however, shrink the forward angular range (characterised by $\sigma_{\text{elast}} / \sigma_{\text{Ruth}} \approx 1$) where breakup events from large impact parameters are prevailing, and they lead to difficulties in achieving the necessary angular accuracy and resolution.

Figure 5 displays the kinematical situation for a typical detector arrangement, as example, for the case of ${}^6\text{Li} \rightarrow \alpha + \text{d}$ breakup at 156 MeV (31,32). The minimum value of the relative fragment energy

$$E_{bc} = \frac{1}{m_b + m_c} \left[m_c E_b + m_b E_c - 2\sqrt{m_b m_c E_b E_c} \cos \Theta_{bc} \right] \quad (3.2)$$

remarkably slowly varying ('magnifying glass effect') in a double-valued way along the kinematic locus $E_b = f(E_c)$ of the (elastic) breakup process: $a + T_{g.s.} \rightarrow b + c + T_{g.s.}$, is limited by the minimum of the relative emission angle Θ_{bc} , reachable by the experimental setup. Thus, the limit in the energy resolution

$$dE_{bc} = \frac{2\sqrt{m_b m_c E_b E_c}}{m_b + m_c} \sin \Theta_{bc} dE_{bc} \quad (3.3)$$

is strongly determined by Θ_{bc} and its uncertainty.

The angular precision and accuracy of the experimental setup needs particular attention if information on the fragment angular distribution is extracted. Since the electromagnetic multipoles contribute with different strengths in capture and Coulomb excitation, the inverse cross sections have to be disentangled, in particular with respect to a non-negligible contributions and interference of electric dipole and quadrupole transitions. Since the ratio

of the E1 and E2 dissociation probabilities depends on the impact parameter (33), a variation of the impact parameter (by the observed scattering angle of the projectile in the forward region) provides, in principle, a possibility to infer corresponding information.

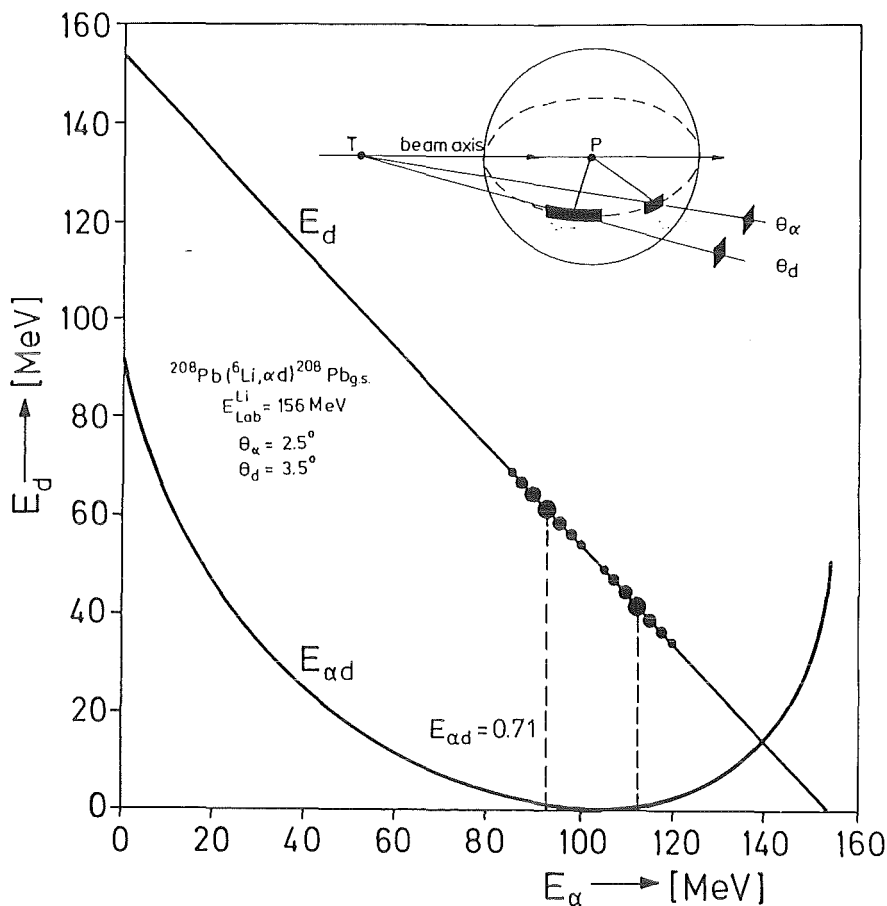


Fig. 5: Kinematic loci of correlated emission of deuterons and α -particles from the ground state of ^{208}Pb . The inset indicates the relation between the laboratory and the center-of-mass system of the decaying projectile. Note: The relative energy of the fragments ($E_{\alpha d}$) shows up with two branches around the minimum (located near the beam-velocity-energies of the fragments).

An alternative source of information is the angular correlation (34) and longitudinal momentum distribution of the fragments, whose determination requires, however, ultimate angular resolution. Recently Esbensen and Bertsch (35) have analysed the effects specified for the example of E1 - E2 interference in the case of Coulomb dissociation of ^8B . It should be noted that the two branches ($v_b > v_c$ and $v_b < v_c$) of the relative energy E_{bc} along the kinematical locus in the $E_b - E_c$ diagram for a fixed laboratory angle pair (Θ_b, Θ_c) (see the example of Figure 5) correspond to different correlated emission angles of the fragments in the decaying projectile. Thus, from a comparison of the differential cross sections along the

two branches and of their asymmetries, information on the fragment angular correlation (for relative energies above the minimum defined by eq. 3.2) can be inferred.

In order to approach the experimental requirements the pilot experiment (31,32), exploring the ${}^6\text{Li} \rightarrow \alpha + d$ breakup at low relative energies, used a specially designed spectrometer setup and applied the split-focal plane detector technique (36, 37) in order to observe the fragment with parallel emission in the extreme forward-angle hemisphere (Figures 6).

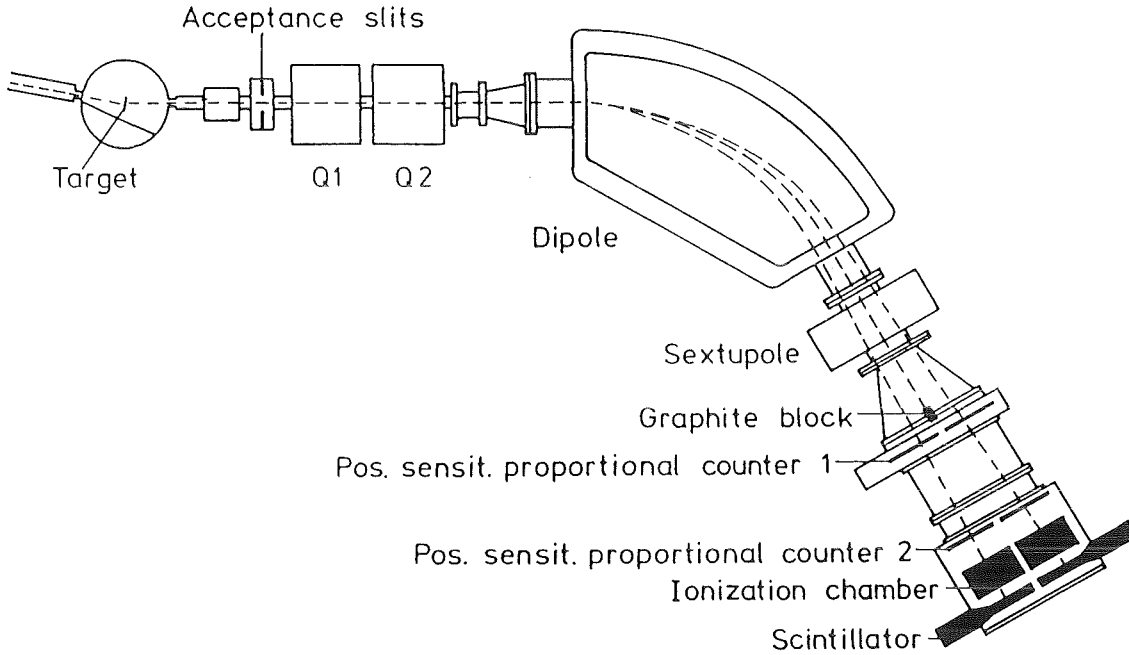


Fig. 6: Schematic view of the magnetic spectrograph „Little John“ with a split detector system for coincident detection of the breakup fragments and ray-tracing of the trajectories (2, 6, 7)

The spectrograph technique strongly minimises problems of conventional detector telescopes: geometric limitations, overloading; reducing the coincidence detection efficiency by the dominance of elastic scattering events. It can be extended for to charged-particle-neutron coincidence measurements by inserting a straight-through port in the focal plane (36).

In various cases of actual interest the experiment has to identify simultaneously particles of very different masses like in the ${}^{14}\text{O} \rightarrow p + {}^{13}\text{N}$ (38, 39), the ${}^{12}\text{N} \rightarrow p + {}^{11}\text{C}$ (10) and the ${}^8\text{B} \rightarrow p + {}^7\text{Be}$ (11) experiments. Figure 7 displays the setup used at GANIL, first for ${}^{14}\text{O}$ dissociation (38) and recently for ${}^{12}\text{N}$ breakup (40). The ${}^{11}\text{C}$ ions emitted from the ${}^{208}\text{Pb}$ target have been observed with magnetic spectrometer SPEG, while the protons are detected with an array of CsI detectors. In the focal plane of the spectrometer, two drift

chambers allowed the determination of the momentum and the emission angle of particles triggering the plastic scintillator. This plastic scintillator measured the energy loss of the heavy fragments and delivered a trigger signal for time-of-flight measurements.

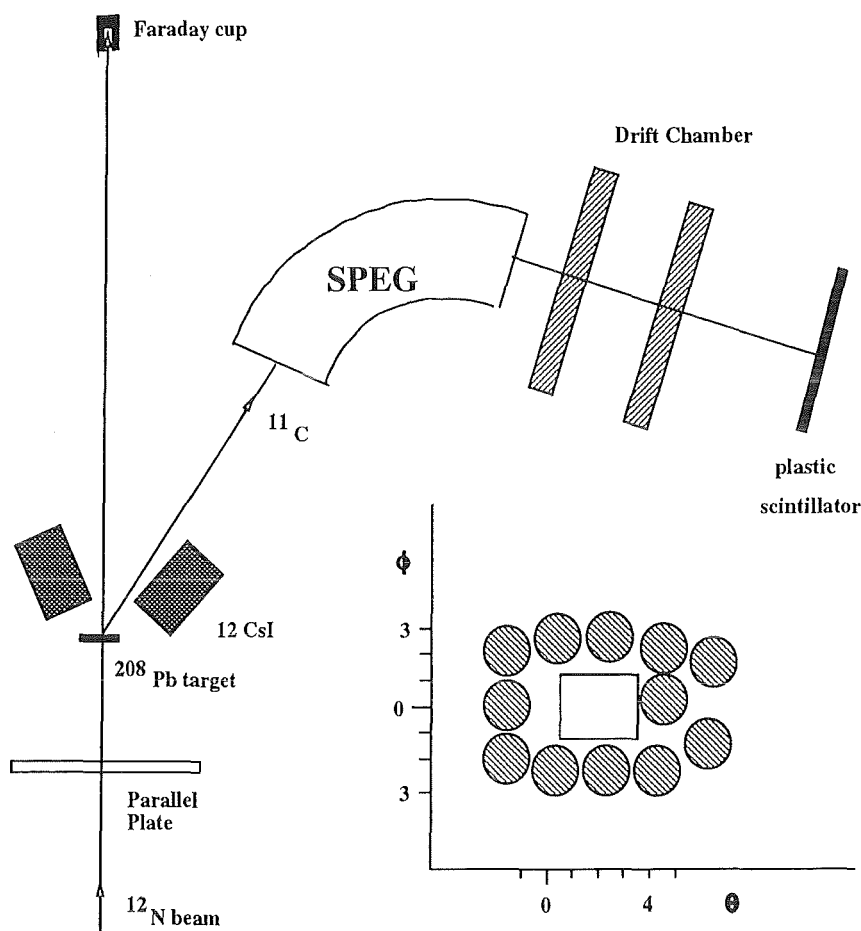


Fig. 7: Detection set-up used at the SPEG spectrometer of GANIL for $^{14}\text{O} \rightarrow ^{13}\text{N} + p$ (8) and $^{12}\text{N} \rightarrow ^{11}\text{C} + p$ (10) breakup experiments. The parallel plate detector upstream from the lead target served for beam intensity determination and beam quality control.

In contrast, at RIKEN (39,41) the fragments of dissociation of ^8B (produced by bombarding a ^7Be target with 91 MeV / amu and analysed with the fragment separator RIPS) are detected by a $\Delta E - E$ plastic scintillator hodoscope. In the arrangement of the ^8B experiment (Figure 8) the ΔE and E plane have been segmented by various strips, so that the hodoscope was divided in 16 segments. The energy of the breakup fragments was determined by time of flight. In order to reduce reactions of the fragments with air nuclei a helium bag has been inserted between target and hodoscope.

Also without using a magnetic spectrograph, a further ^8B dissociation experiment has been started at the National Superconducting Cyclotron Laboratory of the Michigan State

University (42). The fragments are detected by a complex stack of silicon detectors (with a 40×40 Si - strip detector in front) and stopping the high-energy protons in a CsI detector.

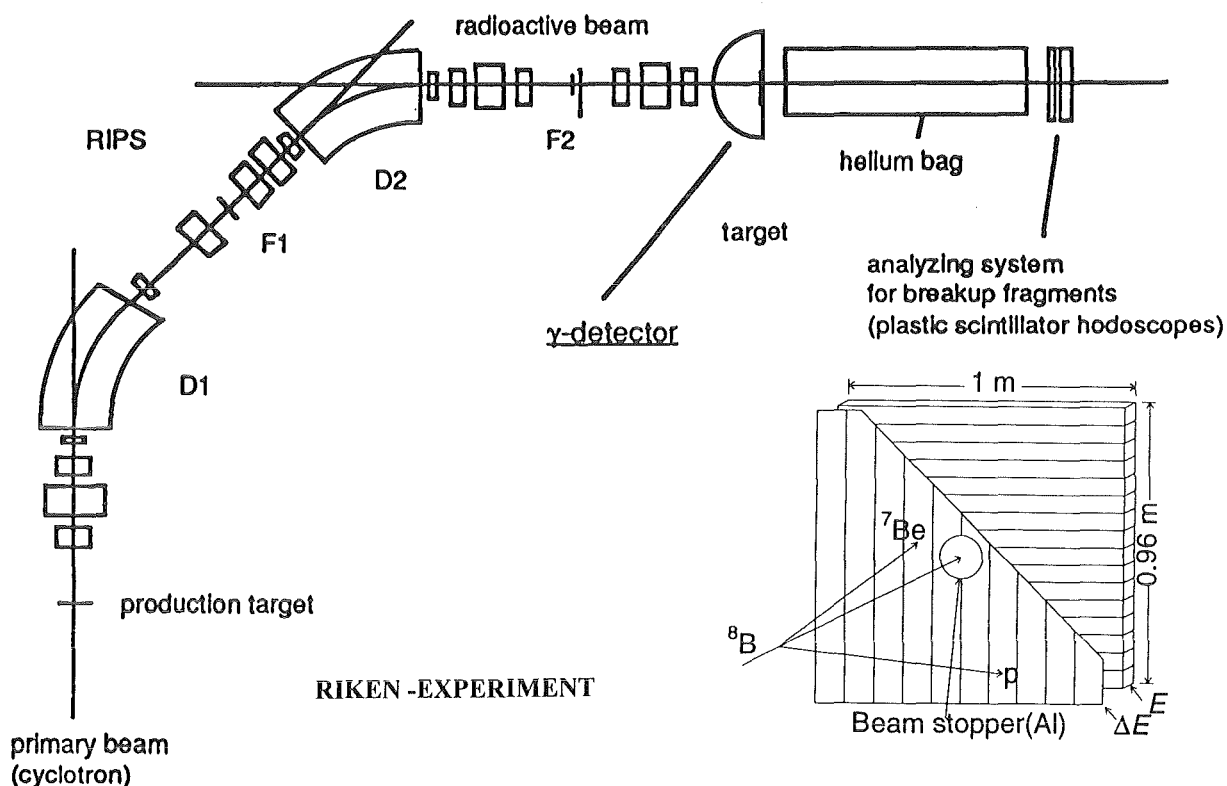


Fig. 8: Scheme of the RIKEN-RIPS radioactive beam facility and the setup of the ^8Be dissociation experiment (11). The inset displays schematically the plastic scintillator hodoscope of an effective area of $1 \cdot 0.96 \text{ cm}^2$. It consists of a 5 mm thick ΔE plane subdivided horizontally into 10 strips and a 6 cm thick E plane segmented vertically into 16 strips.

It has become customary to analyse the performance of the particular experimental arrangement by Monte-Carlo simulations, taking into account effects of energy and angle straggling in the target and detector windows, the detector resolutions, detection efficiencies and the quality of the projectile beam. Actually the restrictions in angular accuracy, energy resolution and the comparatively large minimum values of the relative fragment energies, reachable with in the current experiments with radioactive projectiles are dominantly due to geometrical restrictions of the detector setups and due to the limited quality (emittance) of the secondary beams. Control of the beam quality and energy calibration are major items in approaching the sufficient accuracy of the data.

The situation could be improved by more dedicated experimental arrangements, which prepare economically high-quality beams and allow a flexible application of adequate

spectrometers. A storage-ring facility has been suggested for this possibility (43) and would open a larger field of interesting applications.

4. SPECIFIC FEATURES OF ASTROPHYSICALLY RELEVANT CASES

There are various astrophysical sites where more detailed information on rates of radiative capture reactions is needed. Tab. 2 compiles a number of cases, which seem potentially accessible to the Coulomb dissociation approach, and gives an impression on the field. However, the experimental feasibility and theoretical aspects have to be considered for each particular case separately. This is, because some of the important parameters for Coulomb dissociation are quite different for different cases. E.g., for the ${}^8\text{B} \rightarrow {}^7\text{Be} + \text{p}$ dissociation, the threshold is favourably low. On the other hand, the quality of radioactive beams is generally restricted and this limits the angular and energy resolution. In contrast, an ${}^{16}\text{O}$ beam can certainly be prepared with higher quality, but the rather high breakup threshold of 7.162 MeV (${}^{16}\text{O} \rightarrow \alpha + {}^{12}\text{C}$) and the mixture of E1 and E2 multipole components will certainly complicate the application of the method. Also the astrophysical relevance varies strongly from case to case (sometimes it varies also with time).

On the theoretical side, the main progress since the last review has been in the understanding of higher order, (“post-acceleration“) effects. This was described in Ch. 2. This has a profound influence on the choice of experimental conditions. In order to minimize these effects, the higher the energy, the better it is. Of course, there are other conflicting considerations, like the experimental energy resolution. May be, by varying the beam energy, one can succeed to isolate the effects of higher order.

At various radioactive beam facilities there are now programs to study electromagnetic excitation of bound states by measuring the subsequent γ -decay. In this way, ${}^{11}\text{Be}$ was studied at GANIL (24), the strongly deformed nucleus ${}^{32}\text{Mg}$ was studied at RIKEN (44), and first results on ${}^{36}\text{Ar}$ are reported in (45). Using the theory of electromagnetic excitation, electromagnetic matrixelements ($B(\pi\lambda)$ - values) are extracted from such experiments. We stress at this point that the physics of the presently discussed experiments is the same. The result can be expressed in terms of $B(\pi\lambda)$ - values or, equivalently, astrophysical S-factors. Thus, the same kind of discussion about the reliability of the extracted electromagnetic matrix-elements applies equally to all cases.

Table 2: Radiative capture reactions of interest for light element synthesis accessible by Coulomb dissociation of fast projectiles.

Reaction	$T_{1/2}$ (projectile)	Astrophysical Site	Reference
${}^3\text{He}(\alpha, \gamma) {}^7\text{Be}$ ${}^7\text{Be}(p, \gamma) {}^8\text{B}$ ${}^7\text{Be}(\alpha, \gamma) {}^{11}\text{C}$	53.3 d 770 ms 20.4 m	Solar neutrino problem ${}^3\text{He}$ abundancy	Motobayashi et al. 1994 (71)
${}^4\text{He}(d, \gamma) {}^6\text{Li}$ ${}^6\text{Li}(p, \gamma) {}^7\text{Be}$ ${}^6\text{Li}(\alpha, \gamma) {}^{10}\text{B}$ ${}^4\text{He}(t, \gamma) {}^7\text{Li}$ ${}^7\text{Li}(\alpha, \gamma) {}^{11}\text{B}$ ${}^{11}\text{B}(p, \gamma) {}^{12}\text{C}$ ${}^9\text{Be}(p, \gamma) {}^{10}\text{B}$ ${}^{10}\text{B}(p, \gamma) {}^{11}\text{C}$	stab. 53.3 d stab. stab. stab. stab. stab. 20.4 m	Primordial nucleosynthesis of Li Be B-isotopes	Kiener et al 1989, 1991 (32) Utsunomiya et al. 1990 (47)
${}^7\text{Li}(n, \gamma) {}^8\text{Li}$ ${}^8\text{Li}(n, \gamma) {}^9\text{Li}$ ${}^{12}\text{C}(n, \gamma) {}^{13}\text{C}$ ${}^{14}\text{C}(n, \gamma) {}^{15}\text{C}$ ${}^{14}\text{C}(\alpha, \gamma) {}^{18}\text{O}$	842 ms 178 ms stab. 2.45 s stab.	Primordial nucleosynthesis in Inhomogeneous Big Bang	
${}^{12}\text{C}(p, \gamma) {}^{13}\text{N}$ ${}^{16}\text{O}(p, \gamma) {}^{17}\text{F}$ ${}^{13}\text{N}(p, \gamma) {}^{14}\text{O}$ ${}^{20}\text{Ne}(p, \gamma) {}^{21}\text{Na}$	10 m 65 s 70.6 s 22.5 s	CNO-cycles	Motobayashi et al. 1991 (39), Kiener et al. 1993 (38)
${}^{11}\text{C}(p, \gamma) {}^{12}\text{N}$	11 ms	Hot p-p chain	Lefevbre et al. 1995 (40)
${}^{15}\text{O}(\alpha, \gamma) {}^{19}\text{Ne}$ ${}^{31}\text{S}(p, \gamma) {}^{32}\text{Cl}$	17.2 s 291 ms	rp-process	
${}^{12}\text{C}(\alpha, \gamma) {}^{16}\text{O}$ ${}^{16}\text{O}(\alpha, \gamma) {}^{20}\text{Ne}$ ${}^{14}\text{N}(\alpha, \gamma) {}^{18}\text{F}$	stab. stab. 109.7 m	Helium-burning	Tatischeff et al. 1995 (64) Utsunomiya et al. 1994 (65)

Coulomb excitation for nuclear astrophysics can be viewed as embedded in a large, more general program. We also include a few examples which are of minor importance for nuclear astrophysics, but of relevance from the methodical point of view.

4.1 Coulomb dissociation of ${}^6\text{Li}$ and ${}^7\text{Li}$

The cross section for radiative capture of ${}^4\text{He}$ and d , or t , at energies of the order of 100 keV are of importance for the nucleosynthesis in the expanding universe, a few minutes after the primordial Big Bang. Breakup experiments with stable Li projectiles have played a guiding role in developing the method and working out the salient features (see Ch. 5 of (15)). The pilot experiment performed at the 156-MeV ${}^6\text{Li}$ beam of the Karlsruhe Isochronous Cyclotron, demonstrated the feasibility of the method and observed the direct Coulomb breakup down to rather low relative fragment energies. In the course of these studies the necessary conditions of an successful application have been clarified. The case is also a fortunate test case due to the existence of a well-known resonance at $E_{\alpha d} = 0.71$ MeV, corresponding to the first excited state in ${}^6\text{Li}$ (3^+ ; $E_x = 2.185$ MeV) and as the electromagnetic transition probability $B(E2; 1^+ \rightarrow 3^+)$ is known from independent measurements. The ${}^4\text{He}(d, \gamma){}^6\text{Li}$ capture reaction has been recently reconsidered theoretically in view of a E1 contribution at lower energies. The theoretical analysis is based on a knowledge of the asymptotic normalization coefficient for ${}^6\text{Li} \rightarrow \alpha + d$. Another microscopic calculation was performed in (46). It seems fair to say that more work is needed to resolve these problems. At this point one should remember that, due to the E2 enhancement, the Coulomb dissociation is more sensitive to the E2 than to the E1 part. In the data of (32), no E1 part could be found. In principle, one is also sensitive to E1, mainly by the interference term with E2.

The $(\alpha + t)$ threshold in ${}^7\text{Li}$ is at $E_{\text{thr}} = 2.4678$ MeV. For an impact parameter of $b = 15$ fm and a transition energy of $\hbar\omega = 2.5$ MeV the adiabaticity parameter is given by

$$\xi \cong 0.2 \left(\frac{c}{v} \right) \quad (4.1)$$

Experiments have been performed at ${}^7\text{Li}$ beam energies of 42 to 70 MeV (47). This corresponds to ξ -values of 1.8 and 1.37, respectively. In this region, post-acceleration effects (note the different charge to mass ratio of the fragments α and t) can be substantial

and hard to cope with theoretically. Such objections would be absent at beam energies around 50 MeV/A or more, with the correspondingly lower ξ -values. Under such conditions, an experiment seems worth-while, and amenable to theoretical analysis. Since there are also data for radiative capture, this would also serve as a good test case of the method. Nevertheless, the ${}^7\text{Li} \rightarrow \alpha + t$ breakup experiments can be considered as pioneer experiments in the field.

4.2 Dissociation of ${}^{11}\text{Li}$ and ${}^{11}\text{Be}$

Although these cases seem not to be relevant for nuclear astrophysics, the Coulomb dissociation method was applied to obtain information on electromagnetic transition matrix-elements. It seems appropriate to summarize what lessons can be learned from these cases for the method in general. ${}^{11}\text{Li}$ -Coulomb dissociation was studied at GANIL, RIKEN, MSU, GSI and SATURNE (48). The low lying E1 strength was mapped out, and it is quite well understood in general. Although there is an overall consistency between experimental and theoretical results, the “post-acceleration“ issue is not yet fully under control. Using reasonable assumptions about the structure of the loosely bound ${}^{11}\text{Li}$, the influence of higher order electromagnetic interactions was studied theoretically. Quite different methods were used, and there seems to be a consensus that the post-acceleration effects are smaller than those observed experimentally (49).

The situation with respect to the dissociation ${}^{11}\text{Be} \rightarrow {}^{10}\text{Be} + n$ is quite similar. Due to the presence of one valence neutron only, as compared to the two valence neutrons in the ${}^{11}\text{Li}$ case, ${}^{11}\text{Be}$ seems even more suitable to test the method. The present problems with respect to the excitation of the $\frac{1^-}{2}$ bound state in ${}^{11}\text{Be}$ were already discussed in Ch. 2. The low-lying E1-strength in ${}^{11}\text{Be}$ is mapped out nicely, similar to the situation with ${}^{11}\text{Li}$, there seems to be a post-acceleration effect also (50).

The fact that one can trace out such kind of discrepancies between theory and experiment shows the maturity of the field: there is no room for fiddling around with ill-understood parameters. More studies on the theoretical as well as experimental side will certainly reveal a consistent picture.

4.3 The $^{14}\text{O} \rightarrow ^{13}\text{N} + \text{p}$ Coulomb dissociation

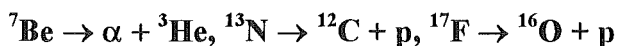
A major change in the classical CNO cycle occurs when the $^{13}\text{N}(\text{p}, \gamma)^{14}\text{O}$ radiative capture process becomes more rapid than the β -decay of ^{13}N . The rate of the capture reaction is essentially determined by the gamma width Γ_γ of the 5.173 MeV 1^- resonance in ^{14}O .

A direct measurement at the Radioactive Beam Facility of Louvain-la-Neuve gave a value of $\Gamma_\gamma = (3.8 \pm 1.2)$ eV (51). It is gratifying that this value compares well with the Coulomb dissociation experiments at RIKEN ($\Gamma_\gamma = (3.1 \pm 0.6)$ eV, (52)) and GANIL ($\Gamma_\gamma = (2.4 \pm 0.9)$ eV, (53)). Further details were already given in (15). In the meantime, the theoretical estimate of higher order electromagnetic excitation, a question raised by Th. Delbar (54) has been published (55). Such effects can safely be neglected for both of the mentioned Coulomb dissociation experiments.

4.4 The $^{12}\text{N} \rightarrow ^{11}\text{C} + \text{p}$ Coulomb dissociation

Hydrogen burning can take place explosively in a variety of sites, e.g. in pregalactic stars formed with ashes of Big Bang or nova explosions. In such a hot p-p mode (56) the $^{11}\text{C}(\text{p}, \gamma)^{12}\text{N}$ reaction is identified to be of particular importance. This reaction is studied in (57) on the basis of a microscopic cluster-model. This is described in (15). Since then, a $^{12}\text{N} \rightarrow ^{11}\text{C} + \text{p}$ Coulomb dissociation experiment has been performed at GANIL (40). From the experimental breakup yield, the radiative width of the 1.19 MeV level in ^{12}N and the spectroscopic factor for the direct proton capture on ^{11}C have been extracted. The radiative width of the 1.19 MeV level is found to be smaller by more than one order of magnitude compared to a recent theoretical calculation (57) but in rough agreement with an estimate by Wiescher et al.

4.5 Some cases, which can also be useful as a test of the method:



The $\alpha(^3\text{He}, \gamma)^7\text{Be}$ reaction is astrophysically relevant. The production of ^7Be is important for the solar neutrino problem. Experimental data as well as theoretical calculations exist. This reaction can also be investigated with the $^7\text{Be} \rightarrow \alpha + ^3\text{He}$ Coulomb dissociation process. The key to a successful experiment will be high beam energies, which will minimize

post-acceleration effects. There are two aspects of such an experiment (58): it can serve as a test case of the method and it can give new information, especially in the low energy region.

As a byproduct of the $^{14}\text{O} \rightarrow ^{13}\text{N} + p$ Coulomb dissociation experiment at RIKEN (52), the $\frac{1^-}{2} \rightarrow \frac{1^+}{2}$ transition to the 2.365 MeV unbound level in ^{13}N was studied. The corresponding $B(E1)$ - value has been known independently before. The good agreement of the two values is another successful test of the method.

Another instructive case would be the $^{17}\text{F} \rightarrow ^{16}\text{O} + p$ Coulomb dissociation. This example also shows clearly the limitations of the method. Good data for the capture reactions $^{16}\text{O}(p, \gamma_0) ^{17}\text{F}$ and $^{16}\text{O}(p, \gamma_1) ^{17}\text{F}(\frac{1^+}{2})$ exist (59). A relevant part of the level scheme of ^{17}F is given in Figure 9.

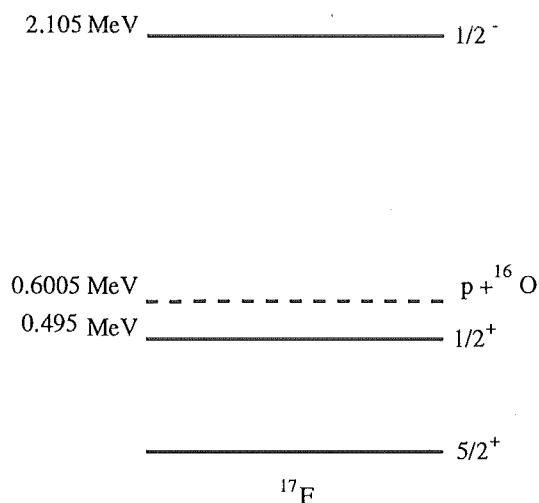


Fig. 9: Part of the ^{17}F level scheme.

We note the following points: The direct radiative capture from the continuum can lead via an E1-transition to the $\frac{5^+}{2}$ ground state as well as to the 1st excited $\frac{1^+}{2}$ state. Only the ground state branch can be studied with the Coulomb excitation method. Since the $p + ^{16}\text{O}$ threshold is only around 600 KeV, this should be a rather good case, with a strong flux of low energy equivalent photons. It should be possible to produce a secondary ^{17}F beam at laboratories like GANIL, MSU, RIKEN or GSI. The corresponding high energies (say ≥ 50 MeV/A) should help to make post-acceleration effects minimal. Note that the mass as well

as the charge to mass ratio are very different for the fragments p and ^{16}O . The $\frac{1^-}{2}$ resonance at $E_x = 3.105$ MeV decays predominantly via E1 to the $\frac{1^+}{2}$ excited state. This cannot be studied with the Coulomb dissociation method. The possibility of a two-step electromagnetic excitation $\frac{5^+}{2} \rightarrow \frac{1^+}{2} \rightarrow \frac{1^-}{2}$ seems rather remote.

4.6 Cases relevant for an inhomogeneous Big-Bang nucleosynthesis

Nonstandard big bang nucleosynthesis leads to the production of ^{14}C , see e.g. (60, 61, 62). This nucleus is of particular importance in these scenarios, since it is a bottleneck for the production of heavier nuclei. There are three possible capture reactions, $^{14}\text{C}(\alpha, \gamma)^{18}\text{O}$, $^{14}\text{C}(p, \gamma)^{15}\text{N}$ and $^{14}\text{C}(n, \gamma)^{15}\text{C}$. The astrophysical rates for the first two of them are reliably known. More information is needed for the neutron capture reaction. It is known experimentally that $\sigma_{\text{thermal}} < 1 \mu\text{b}$. The relevant level scheme is shown in Figure 10.

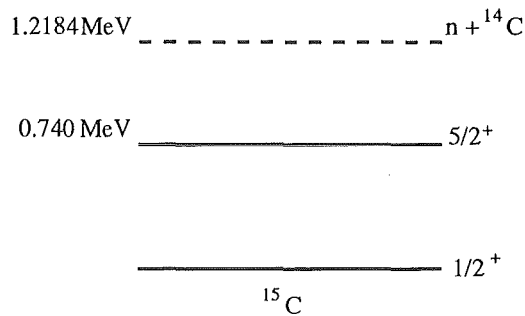


Fig. 10: Part of the ^{15}C level scheme.

We suggest that Coulomb dissociation of $^{15}\text{C} \rightarrow ^{14}\text{C} + n$ could provide useful information.

At the lowest neutron energies, the $S_{1/2} \xrightarrow{\text{E2}} \frac{5^+}{2}$ capture to the first excited state will be dominant. However, as was pointed out in (61) the higher energy region is relevant for

astrophysics. In this region, there are the $p_{3/2} \xrightarrow{E1} \frac{5^+}{2}$ and $p_{3/2}, p_{1/2} \xrightarrow{E1} \frac{1^+}{2}$ transitions. The Coulomb dissociation approach can be used to study the $\frac{1^+}{2} \xrightarrow{E1} p_{1/2}, p_{3/2}$ excitation into the continuum. The Q-value is comparatively low, and the method should work well. At sufficiently high beam energies, say several tens of MeV/amu, post-acceleration effects should be under control.

4.7 Aspects and challenge of dissociation of ^{16}O

Helium burning of $^{12}\text{C} (\alpha, \gamma) ^{16}\text{O}$ at thermonuclear energies is a key process for the evolution of massive stars and for the nucleosynthesis of ^{16}O and heavier elements up to Fe. However, the cross section at the effective energy of about 300 keV, estimated to be in the order of 10^{-8} nb, is far off the reach of indirect measurements. In spite of enormous efforts the lower limits of direct capture measurements lie around 1 MeV (63). Theoretical extrapolations are particularly difficult and uncertain due to a rather complex situation arising from a superposition of E1 and E2 capture processes. In addition at energies below 1 MeV these processes result from the interference of sub-threshold resonances (1^- ; 7.117 MeV and 2^+ ; 6917 MeV) of unknown α -spectroscopic factors with a resonance at higher excitation energies resonances (1^- ; 9.552 MeV) in ^{16}O and direct E2 capture. Thus, any extrapolation to the lower energy and subfemtobarn range of the cross-section appears to be rather delicate and uncertain.

Due to the astrophysical importance, from the very beginning (13) the application of the Coulomb dissociation method has been proposed for improving the present knowledge. The considerations about experimental feasibility, the complicating features and the necessary conditions have put forward interesting modifications of the original methodical concept (64, 65). The main complications arise from following features:

- (i) Due to the comparatively high-lying $\alpha + ^{12}\text{C}$ threshold of 7.16 MeV rather large projectile energies of about 500 MeV / amu are required in order to produce a sufficiently large intensity of correspondingly high-energy (quasi-real) photons, enhancing the electromagnetic process to be dominating the ^{16}O breakup. Such an attempt implies extreme difficulties to achieve the necessary angular accuracy in the extreme forward angle hemisphere, in particular for angular correlation studies.

- (ii) At bombarding energies in the order 100 MeV/amu E2 excitation prevails over E1 excitation (34, 66), so that Coulomb excitation gives access mainly to the E2 capture cross section only. This restriction, however, could be of special interest and complementary to the information extracted from measurements of the β -delayed α -decay of ^{16}N (9, 67).
- (iii) Moreover, in the considered energy range, considerable contributions and interferences from nuclear breakup have to be expected. In view of future experimental plans under discussion at GANIL and RIKEN, Tatischeff et al. (64) and Utsunomiya et al. (65) propagate an approach which handles electromagnetic and nuclear excitation on equal footing and attempts to identify and to isolate both contributions by use of detailed coupled channel analyses of the nuclear-Coulomb interference and of the fragment-angular distributions. While the ORSAY-GANIL group bases the calculations on a phenomenological model of the nuclear interaction with a flexible parametrization of the formfactors and transition strengths, Utsunomiya et al. (65) advocate a microscopic interaction model as generator specifying consistently the coupling strengths for extensive CDCC („Continuum Discretized Coupled Channels“) studies (68).

The approach of using the unavoidable nuclear interference as a vehicle to reveal the electromagnetic part is of considerable interest, and the extension to continuum couplings would be certainly a progress of significance, especially when the electromagnetic continuum can be treated with equal accuracy.

4.8 $^8\text{B} \rightarrow ^7\text{Be} + \text{p}$ Coulomb dissociation and the Solar Neutrino Problem

The solar neutrino problem is still with us (see e.g. (69), and further references given there). There are the Davis-experiments with the ^{37}Cl detector, and the Kamiokande experiments, based on electron-neutrino scattering. They are mainly sensitive to the high energy neutrinos. Most of these high energy neutrinos result from ^8B β^+ decay. There is a deficit of detected neutrinos, which one can call the ^8B solar neutrino problem. Solar neutrino results from the GALLEX collaboration, which are also sensitive to the low energy part of the spectrum, were given recently (70). There is also a deficit and possibly another solar neutrino problem. One can say that the solar neutrino problem has many difficult aspects,

and many possible solutions, ranging from fundamental neutrino physics (like MSW effect) to rather sobering aspects of nuclear astrophysical reaction rates.

${}^8\text{B}$ is formed in the ${}^7\text{Be} (p, \gamma) {}^8\text{B}$ radiative capture reaction. Thus the astrophysical S-factor of this reaction is of direct importance for the ${}^8\text{B}$ solar neutrino problem.

The Coulomb dissociation of ${}^8\text{B}$ can well be used to study this question: ${}^8\text{B}$ can be produced as an exotic secondary beam at intermediate energies. The ${}^8\text{B} \rightarrow {}^7\text{Be} + p$ threshold is very low, therefore the equivalent photon flux is high, and competition from nuclear excitation is very small. Higher order electromagnetic effects can be kept under control.

In (71) the Coulomb dissociation method was applied to this problem for the first time. In a first attempt, an astrophysical S-factor was extracted, which was rather low, as compared to direct radiative capture measurements. Even before the RIKEN experiment could get published, it was noted (72) that it is important to take the E2 contribution into account in an analysis of the Coulomb dissociation results. The problem is well identified by now (73, 74), a discussion is also given by G. Taubes in Science (75). As it will be discussed below, many theories to have studied the analysis of ${}^8\text{B}$ Coulomb dissociation experiments in a wider context. There is a general consensus that it is necessary and possible to disentangle the E1 and E2 contributions by means of their characteristic angular distributions. There could be something to worry about in principle: ${}^8\text{B}$, as produced by high energy fragmentation, could be spin-polarized. It remains to be studied how this can influence the angular correlations. Further experimental results are eagerly awaited.

A kinematically complete experiment on ${}^8\text{B} \rightarrow {}^7\text{Be} + p$ Coulomb dissociation was performed at NSCL/MSU (76) and is presently being analysed. A ${}^8\text{B}$ Coulomb dissociation experiment at around 200 MeV/A will be done at GSI this year (77). At such high projectile velocities, it should be possible to see the M1-resonance. This would be a nice check of the experimental method. It will be very interesting to see the analysis of these experiments in terms of astrophysical S-factors. Of course, all these experiments done at different experimental conditions (incident energy, scattering, angles, etc.) should yield the same astrophysical S-factor. This is a very valuable consistency check.

On the theoretical side, the problems of analysing ${}^8\text{B}$ Coulomb dissociation experiments have been studied by various authors (30, 78, 79, 80, 81, 35). Despite different methods, there is a remarkable consensus on all important issues. It can be summarized as follows:

- (i) a model-independent separation of E1 and E2 components is possible by a careful study of angular distributions
- (ii) at RIKEN or higher energies, nuclear effects are virtually negligible. Essentially, this is due to the rather large impact parameters, which are relevant for Coulomb dissociation. In turn this is related to the low $p+{}^7\text{Be}$ threshold (in marked contrast to the ${}^{16}\text{O}$ case discussed in the previous section)
- (iii) higher order electromagnetic effects become relevant only at incident energies well below the RIKEN energies. This is the conclusion of three different approaches: higher order perturbation theory (30), numerical integration of the time-dependent Schrödinger equation (35) and a coupled channels approach (80).

In conclusion, it can be said that the pioneering experiment at RIKEN (71) showed the feasibility of the method, all the theoretical tools to analyse these experiments are available. So, a reliable value of the astrophysical S-factor by means of the Coulomb dissociation method can soon be expected. It remains to be seen, what the impact on the ${}^8\text{B}$ solar neutrino problem will be.

5. CONCLUDING REMARKS

Peripheral collisions of high-energy heavy ions, passing each other in distances without nuclear contact and dominated by electromagnetic interactions are an important tool of nuclear physics research. The intense source of quasi-real photons, exchanged by the collision partners, has opened a large horizon of related problems and new experimental possibilities to investigate efficiently photo-interactions with nuclei (single- and multiphoton excitations and electromagnetic dissociation) and particle production in the electromagnetic field (Primakoff effect (10)).

In this prospect the Coulomb dissociation approach of nuclear astrophysics is focussed to studies of electromagnetic dissociation of fast charged projectiles in the field of a large Z -nucleus, observing the emerging fragments with near parallel emission (in the very forward angle direction) i.e. with very small relative energies. This process approximates the time-reversed process of a particular class of nuclear reactions of astrophysical interest: photocapture processes. Since this access to 'hard-to-measure' cross sections has been proposed (13) as tool of laboratory nuclear astrophysics the understanding of the

methodical basis has considerably progressed in the course of a number of experiments, attacking interesting problems, and by detailed investigations of the theoretical implications of the approach. In general the main complications arise (i) from contributions of nuclear breakup resulting from grazing collisions and interfering with Coulomb trajectories with larger impact parameters and (ii) from final state effects (higher order excitations in the continuum of the emerging fragments).

These effects are well identified and their importance and influence have to be discussed specifically in each particular case, in order to establish the experimental conditions of minimum distortions. With this view the compilation of cases in Table 2, potentially accessible for the approach, has to be considered. It demonstrates the impact to studies of astrophysical problems at the frontier of current research. The dissociation of ${}^8\text{B}$ and its relevance to the solar neutrino problems is a particular example of far-reaching interest.

With the advent of radioactive ion beams of moderate intensity, the large cross sections for Coulomb breakup make the method particularly interesting for studies of capture reactions involving radioactive nuclei. The cases of ${}^{13}\text{N} (p, \gamma) {}^{14}\text{O}$ (38,39) ${}^{11}\text{C} (p, \gamma) {}^{12}\text{N}$ (40) and ${}^7\text{Be} (p, \gamma) {}^8\text{B}$ (71) are examples indicating the progress in experiment and theory. Nevertheless there are quests for improvements in the future, experimentally by more dedicated high-resolution detection facilities with improved quality of projectile beams, theoretically by a more general and practical approach of handling higher-order processes with a quantitative identification in the analyses.

A promising extension and modification of the method is under discussion in context of Coulomb breakup of ${}^{16}\text{O}$ (64,65) as access to the astrophysically important cross section of the ${}^{12}\text{C} (\alpha, \gamma) {}^{16}\text{O}$ reaction in the energy range of $E_{\alpha d} = 300$ keV. It has been emphasized (64) by detailed calculations that the capture cross section can be deduced in presence of interferences of the nuclear contributions, if the experimental layout allows sufficiently precise measurements of the fragment angular distributions.

We thank for interesting discussions, valuable informations and encouragement of many colleagues and are particularly grateful for useful comments of P. Aguer, C.A. Bertulani, M. Gai, S. Hirzebruch, N. Iwasa, J. Kiener, K.H. Langanke, T. Motobayashi, Y. Sakuragi, C. Samanta, G. Schatz, L. Trache, D. Trautmann, S. Typel and H. Utsunomiya. The help of A. Mündel and S. Burkhardt with some of the figures is gratefully acknowledged.

LITERATURE

1. Fowler WA. 1975. *Rev. Mod. Phys.* 56: 149
2. Rolfs C, Rodney WS. Cauldrons in the Cosmos. Chicago - London: University of Chicago, press
3. Fiorentini G, Kavanagh RW, Rolfs C. 1995. *Z. Phys.* A350: 285
4. Dunbar DNF, Pixley RE, Wenzel WA, Wahling W. 1953. *Phys. Rev.* 92: 64
5. Hoyle F, Dunbar DNF, Wenzel WA, Wahling W. 1953. *Phys. Rev.* 92: 1095
6. Hoyle F. 1954. *Astrophys. J. Suppl.* 1: 1
7. Ji X, Filippone BW, Humblet J, Koonin SE. 1990. *Phys. Rev.* C41: 1736
8. Humblet J, Filippone BW, Koonin SE. 1991. *Phys. Rev.* C44: 2530
9. Buchmann L, et al. 1993. *Phys. Rev. Lett.* 70: 726
10. Primakoff H. 1951. *Phys. Rev.* 3: 889
11. Alder K, Winther A. 1975. Electromagnetic Excitation. Amsterdam: North-Holland
12. Rebel H. 1985. Workshop on Nuclear Reaction Cross Sections of Astrophysical Interest. Kernforschungszentrum Karlsruhe, internal report
13. Baur G, Bertulani CA, Rebel H. 1986. *Nucl. Phys.* A459: 188
14. Srivastava DK, Rebel H. 1986. *J. Phys. G: Nucl. Phys.* 12: 717
15. Baur G, Rebel H. 1994. *J. Phys. G: Nucl. Part. Phys.* 20: 1
16. Bethe HA, Jackiw RW. 1968. Intermediate Quantum Mechanics. Second Edition, A. Benjamin, Inc. New York, Amsterdam
17. Winther A, Alder K. 1979. *Nucl. Phys.* A319: 518
18. Bertulani CA, Baur G. 1986. *Nucl. Phys.* A458: 725
19. Bertulani CA, Baur G. 1988. *Physics Reports* 163: 299
20. Aleixo ANF, Bertulani CA. 1989. *Nucl. Phys.* A505: 448
21. Bertulani CA, Nathan AM. 1993. *Nucl. Phys.* A554: 158
22. Mündel A, Baur G, Typel S. in preparation

23. Typel S, Baur G. 1995. Phys. Lett. B356: 186
24. Anne R, et al. 1995. Z. Phys. A352: 397
25. Bertulani CA, Canto LF, Hussein MS. 1995. Phys. Lett. B353: 413
26. Bertulani CA, Bertsch GF. 1994. Phys. Rev. C49: 2839
27. Esbensen H, Bertsch GF, Bertulani CA. 1995. Nucl. Phys. A581: 107
28. Kido T, Yabana K, Suzuki Y. 1994. Phys. Rev. C50: R 1276
29. Typel S, Baur G. 1994. Nucl. Phys. A573: 486
30. Typel S, Baur G. 1994. Phys. Rev. C50: 2104
31. Kiener J, Gils HJ, Rebel H, Baur G. 1989. Z. Phys. A 332: 359
32. Kiener J, Gils HJ, Rebel H, Zagromski S, Gsottschneider G, Heide N, Jelitto H, Wentz J, Baur G. 1991. Phys. Rev. C 44: 2195
33. Baur G, Bertulani CA, Rebel H. 1986. In Weak and Electromagnetic Interactions in Nuclei. ed. HV Klapdor, p. 980. New-York - London - Paris - Tokyo: Springer
34. Baur G, Weber M. 1989. Nucl. Phys. A 531: 685
35. Esbensen H, Bertsch GF. 1995. Phys. Lett. B 359: 13
Esbensen H, Bertsch GF. to be published
36. Utsunomiya H, Lui YW, Schmitt RP. 1989. Nucl. Instr. Meth. A 278: 744;
Gils HJ, Kiener J, Zagromski S, Rebel H. 1986. KfK-Report 4159,
Kernforschungszentrum Karlsruhe
37. Gsottschneider G. 1990 KfK-Report 4803, Kernforschungszentrum Karlsruhe
38. Kiener J, Lefebvre A, Aguer P, Bacri CO, Bimbot R, et al. 1993. In Radioactive Nuclear Beams, Sect. 4, 2nd Conf. on Radioactive Nuclear beams, Louvain-la-Neuve. 1991. p. 311 - Nucl. Phys. A 552: 63
39. Motobayashi T, Takei T, Kox S, Perrin C, Merchez F, et al. 1991. Phys. Lett. B 264: 259
40. Lefebvre A, Aguer P, Kiener J, Bogaert G, Coc A, et al. 1995. Nucl. Phys. A 595: 69
41. Motobayashi T, Iwasa N, Ando Y, Kurokawa M, Murakami H, et al. 1994. Phys. Rev. Lett. 73: 2680;

- Iwasa N. 1994. Proc. Tours Symposium on Nucl. Physics II, August 30 - September 2, 1994. ed. H Utsunomiya, M Ohata, J Galin, G Münzenberg, p. 68. Singapore - New Jersey - London - Honkong: World Scientific
42. Hirzebruch S, Austin SM. 1995 private communication;
Kelley JH, Austin SM, Azhari A, Bazin D, Brown JA, et al. 1994. Annual Rep. NSCL-MSU, p. 65
43. Gils HJ, Heck D, Rebel H, Schatz G. 1986. Laboratory note, Kernforschungszentrum Karlsruhe (unpublished);
Baur G, Rebel H. 1994. Proc. Tours Symposium on Nucl. Physics II, August 30 - September 2, 1994. ed. H Utsunomiya, M Ohata, J Galin, G Münzenberg, p. 55. Singapore - New Jersey - London - Honkong: World Scientific
44. Motobayashi T. et al. 1995. Phys. Lett. B346: 9
45. GSI Scientific Report. GSI 34-1. R. Schubert et al. p. 34
46. Ryzhikh GG, et al. 1995. Phys. Rev. C51: 3240
47. Ajzenberg-Selove F. 1988. Nucl. Phys A490: 1
48. Blank B, et al. 1993. Nucl. Phys. A555: 408
49. Ieki K, et al. 1993. Phys. Rev. Lett. 70: 730
50. Nakamura T, et al. 1994. Phys. Lett. B331: 296
51. Decroock P, et al. 1991. Phys. Rev. Lett. 67: 808
52. Motobayashi T, et al. 1991. Phys. Lett. 264B: 259
53. Kiener J, et al. Nucl. Phys. 1993. Nucl. Phys. A552: 63
54. Delbar T. 1993. Phys. Rev. C47: R14
55. Typel S, Baur G. 1994. Phys. Rev. C49: 379
56. Wiescher M, Görres J, Graff S, Buchmann L, Thielemann FK. 1989. Astrophys. J. 343: 352
57. Descouvemont P, Baraffe I. 1990. Nucl. Phys. A514: 66
58. Motobayashi T. private communication

59. Rolfs C. Nucl. Phys. 1973. A217: 29
60. Wiescher M, Görres J, Thielemann FK. 1990. Astrophys. J 363: 340
61. Kajino T, Mathews GJ, Fuller GM. 1990. Astrophys. J. 364:7
62. Malaney RA, Mathews GJ. 1993. Phys. Rep. 229: 145
63. Ouellet JML, Evans HC, Lee HW, Leslie JR, Mac Arthur JD, et al. 1992. Phys. Rev. Lett. 69: 1896
64. Tatischeff V, Kiener J, Aguer P, Lefebvre A. 1995. Phys. Rev. C 51: 2789
Tatischeff V, Kiener J, Aguer P, Angulo-Perez C, et al. 1994. Tours Symposium on Nucl. Physics II, Tours, France, August 30 - September 2, 1994, p. 101, eds. Utsunomiya H, Ohta M, Galin J, Münzenberg G.
65. Utsunomiya H, Hirabayashi M, Hirai M, Ichihara T, et al. 1994. Tours Symposium on Nucl. Physics II, Tours, France, August 30 - September 2, 1994, p. 132, eds. Utsunomiya H, Ohta M, Galin J, Münzenberg G.
66. Shoppa TD, Koonin SE. 1992. Phys. Rev. C46: 382
67. Zhao Z, France RH, Lai KS, Rugari SL, Gai M, Wilds EL. 1993. Phys. Rev. Lett. 70: 2066.
Buchmann L, Azuma RE, Barnes CA, d'Auria JM et al. 1993. Phys. Rev. Lett 70: 726
68. Hirabayashi Y, Sakuragi Y. 1994. Tours Symposium on Nucl. Physics II, Tours, France, August 30 - September 2, 1994, p. 118, eds. Utsunomiya H, Ohta M, Galin J, Münzenberg G.
69. Bahcall JN. 1995. Nucl. Phys. B (Proc. Suppl.) 43: 41
70. GALLEX Collaboration. 1995. Phys. Lett. B357: 237
71. Motobayashi T, et al. 1994. Phys. Rev. Lett. 73: 2680
72. Langanke K, Shoppa TD. 1994. Phys. Rev. C49: R 1771
73. Gai M, Bertulani CA. 1995. Phys. Rev. C52: 1706
74. Langanke K, Shoppa TD. 1995. Phys. Rev. C52: 1709
75. Taubes G. 1994. Science Vol. 226: 1157
76. Hirzebruch S. private communication

77. Sümmerer K, et al. GSI Darmstadt, experiment proposal, accepted
78. Bertulani CA. 1994. Phys. Rev. C49: 2688
79. Bertulani CA. 1995. Nucl. Phys. A587: 318
80. Bertulani CA. 1996. GSI-preprint: 05-Januar 1996
81. Shyam R, Thompson IJ, Dutt-Mazumder AK. Phys. Lett. B: in press